

THESIS FOR THE DEGREE OF LICENTIATE OF ENGINEERING

Varestraint Weldability Testing of Cast Superalloys

Sukhdeep Singh



Department of Industrial and Materials Science
CHALMERS UNIVERSITY OF TECHNOLOGY
Gothenburg, Sweden

Varestraint Weldability Testing of Cast Superalloys
Sukhdeep Singh

© Sukhdeep Singh, 2018

Technical report no IMS-2018-7

Department of Industrial and Materials Science
Chalmers University of Technology
SE-412 96 Gothenburg
Sweden
Telephone + 46 (0)31-772 1000

Printed by Chalmers Reproservice
Gothenburg, Sweden 2018

Varestraint Weldability Testing of Cast Superalloys

Sukhdeep Singh

Department of Industrial and Materials Science
Chalmers University of Technology

Abstract

Precipitation hardened Ni- and Ni-Fe- based superalloys, used in hot structural components for aero engines, are subjected to hot cracking phenomena during manufacturing and specifically in welding. This type of cracking involves metallurgical reactions from the liquid phase in concomitance to weld restraints. Hot cracking is more pronounced during the welding of cast superalloys compared to its wrought counterparts owing to the larger inhomogeneity in the cast material. Cast structural components must therefore undergo a hot isostatic pressing (HIP) treatment prior to welding for closing any pores from the casting process and homogenizing the material. The current study is about the effect of two HIP treatments commonly employed in the aerospace industry on the weldability of the cast Alloy 718. Moreover, the weldability of the recently introduced cast version of ATI[®] 718Plus[™] is also addressed, including the assessment of five different pseudo-HIP treatments and the weldability of the two cast superalloys is compared. Testing was conducted using the Varestraint (Variable-Restraint) weldability testing technique, where test plates were welded by a robot and at the same time bended to achieve external restraint. Welding and test parameters were the same for all the conditions. The hot cracking susceptibility of cast Alloy 718 was found to be worse with increasing HIP treatment temperature. It was found that HIP treatment conducted at 1190°C/4h gave higher crack susceptibility than the one at 1120°C/4h. Cast ATI[®] 718Plus[™] was heat treated using short dwell heat treatments for 4h at 1120°C, 1160°C and 1190°C and long dwell heat treatments for 24h at both 1120°C and 1190°C, respectively. The cracking susceptibility was found to be related to the heat treatment dwell time rather than the temperature. The heat treatment at 4h dwell time exhibited lower amount of cracking than the 24h dwell heat treatment. Considering the comparative heat treatments at 1120°C/4h and 1190°C/4h, the new cast superalloy ATI[®] 718Plus[™] was found to have lower cracking susceptibility than the cast Alloy 718.

Keywords: HIP, Varestraint, Welding, Hot Cracking, Cast Superalloys, Alloy 718, ATI[®] 718 Plus[™]

Preface

This licentiate thesis is based on the work performed in the Department of Industrial and Materials Science at Chalmers University of Technology and at the Division of Welding Technology at University West between November 2015 and May 2018 under the supervision of Associate Professor Joel Andersson.

The thesis consists of an introductory part followed by two appended papers.

List of appended papers

Paper I: Hot cracking in cast Alloy 718

Sukhdeep Singh and Joel Andersson

Science and Technology of Welding and Joining, Accepted for publication, available online.

<https://doi.org/10.1080/13621718.2018.1429238>

Paper II: Vareststraint weldability testing of cast ATI[®] 718 Plus[™] – A comparison to cast Alloy 718

Sukhdeep Singh and Joel Andersson

Submitted for journal publication

Contribution to the appended papers

Paper I: Joel Andersson planned the study. The author planned and executed the microstructural investigations, analysed the results and wrote the paper with input from the co-author.

Paper II: Joel Andersson planned the study. The author planned and executed part of the Vareststraint testing with the help of Mr Kjell Hurtig, did the microstructural investigations, analysed the results and wrote the paper with input from the co-author.

Papers not appended to the thesis

Paper 1: Review of hot cracking phenomena in austenitic stainless steels
Sukhdeep Singh and Joel Andersson

7th International Swedish Production Symposium, SPS16, Lund, Sweden, October 25–27, 2016.

Swedish Production Academy, 2016. p. 1-7.

Paper 2: Investigation on effect of welding parameters on solidification cracking of austenitic stainless steel 314

Sukhdeep Singh and Joel Andersson

Accepted for presentation at: 8th Swedish Production Symposium, SPS 2018, 16-18 May 2018,

Stockholm, Sweden

Paper 3: Vareststraint weldability testing of ATI® 718Plus® - Influence of eta phase

Sukhdeep Singh, William Fransson, Joel Andersson, Anssi Brederholm and Hannu Hänninen

Accepted for presentation at: Superalloy 718 & Derivatives conference 2018, 3-6 June, Pittsburgh,

USA.

Table of Contents

1. Introduction	1
1.1. Aim	2
2. Cast Superalloys	3
3. Hot Cracking	5
3.1. Solidification cracking	5
3.2. Heat affected zone liquation cracking	8
4. Experimental Methods	11
4.1. Materials and heat treatments	11
4.2. Vareststraint weldability testing	12
4.3. Sample preparation and characterization	13
5. Summary of Appended Papers	15
5.1. Hot cracking in cast Alloy 718 (Paper I)	15
5.2. Vareststraint weldability testing of cast ATI® 718 Plus™ – A comparison to cast Alloy 718 (Paper II)	17
6. Conclusions	21
7. Future Work	23
8. Acknowledgements	25
References	27

1. Introduction

Nickel and Ni-Fe based superalloys are preferably employed in the hot structural components of aero engines because of their high temperature mechanical strength, corrosion and oxidation resistance. The Ni-Fe based Alloy 718, which was developed in the 1960's [1], is still the most widely used superalloy. It quickly became the work-horse alloy in aerospace applications due to its inherent resistance towards a solid-state cracking phenomenon known as strain age cracking but also owing to the availability in cast form, which was possible due to the development of vacuum melting technology [2]. However, it is limited to relatively low operating temperature of $\sim 650^{\circ}\text{C}$. To meet the demand from the aerospace industry for improved efficiency, the Ni-based ATI[®] 718Plus[™] was introduced about a decade ago. The change to the more stable precipitation strengthening phase, gamma prime (γ') instead of gamma double prime (γ'') as for Alloy 718, by means of careful alloy engineering while maintaining the similarity in fabricability to that of Alloy 718, led to the development of this alloy that could operate at about 705°C [3]. A cast version of ATI[®] 718Plus[™] is now under development to be employed in large structural components [4].

Welding is an important process in the manufacturing chain. The recent trend in the aerospace industry is to join small castings and sheets together instead of single piece castings. This allows for weight reduction and reduces manufacturing costs [5]. The wide range of alloying elements being part of the chemical stew can often lead to microstructural reactions during welding which in turn can cause cracking. This type of a phenomenon is known as hot cracking and occurs when liquid films decrease the ductility during the final stages of solidification in concurrence with strains developed due to the thermal cycling. A thorough understanding of the metallurgy is therefore important as cracking can lead to further complications in the workshop, requiring additional intervention by repair welding.

Cast components often undergo homogenization heat treatments prior to welding. When it comes to cast components for structural applications it is common that they undergo hot isostatic pressing (HIP) treatment to reduce porosity and segregation, which in turn are known to be detrimental to both mechanical properties as well as weldability. In the current study, Variable Restraint (Variable Restraint) weldability testing is applied for investigating the effect of two commonly employed HIP treatments on the hot cracking susceptibility of cast Alloy 718. Further, the weldability of the relatively new superalloy, cast ATI[®] 718Plus[™], is also studied and compared to that of cast Alloy 718.

1.1.Aim

The aim of research has been to investigate the hot cracking susceptibility of cast superalloys by means of Varestraint weldability testing. More specifically, the following research objectives have been formulated:

- To investigate hot cracking susceptibility of cast Alloy 718 involving the comparison of two post HIP treatments at 1120°C and 1190°C at 4h
- To investigate the hot cracking susceptibility of the relatively new cast ATI® 718Plus™, involving the role of different post pseudo-HIP treatments at 1120°C, 1160°C, 1190°C at 4h and 1120°C, 1190°C at 24h
- To compare the hot cracking susceptibility of cast Alloy 718 and cast ATI® 718Plus™

2. Cast Superalloys

The chemical composition of superalloys consists of 12 to 15 different elements, which make the microstructure complex. The elements included are Ni, Fe, Cr, Mo, Nb, Ti, Al, Co, Cu, W, C, Si, S, B and P. Each of these elements has a specific role: elements such as Fe, Co, Cr, Mo confer the solid solution strengthening of the gamma matrix. The elements Ni, Al and Ti are known to form the γ' phase, while Ni and Nb form the γ'' phase. Different type of carbides are expected to form. The commonly known ones are primary MC (containing Nb, Ti) as well as secondary carbides like $M_{23}C_6$ (containing Cr, Mo) and M_6C (with Mo, W). The coarse primary carbides are generally considered detrimental for the mechanical properties, however, the secondary carbides, when uniformly dispersed along the grain boundaries as discrete precipitates, can inhibit grain boundary sliding and consequently improve the strength. Apart from the strengthening phases and carbides, some Ni-Fe base superalloys can also contain topologically close packed (TCP) phases such as σ , μ and Laves. The TCP phases are generally considered detrimental when present along the grain boundaries in plate like morphology and can act as source of crack initiation. Precipitation of other phases along the grain boundaries, such as η and δ , are known to be very effective for grain size control [6]. Table 1 summarises the type of precipitates and their chemistry as present in Ni- and Ni-Fe based superalloys.

Table 1. Commonly found precipitates in Ni- and Ni-Fe based superalloys [6], [7]

Phase	Crystal structure	Ni	Fe	Cr	Mo	Al	Ti	W	Co	Ta	Nb	Cl	Nb	B	Si	S
Matrix		x	x	x	x	x		x	x	x						
γ'	fcc	x				x	x									
γ''	bct	x									x	x				
MC	cubic			x	x		x	x		x	x					
$M_{23}C_6$	fcc		x	x	x			x	x							
M_6C	fcc	x			x			x	x							
δ	orthor.			x							x			x		
σ	tetrag.	x	x	x	x				x							
η	hcp	x		x			x				x					
μ	rhomb.							x	x							
Laves	hexagonal		x		x		x		x		x				x	
M_3B_2	tetrag.			x	x	x				x	x			x		
MN	cubic			x	x		x				x					

The Ni-based superalloy castings intended for hot sections in aircraft applications are produced by investment casting under vacuum in order to avoid oxidation of reactive elements. This technique uses a pattern made out of wax or plastic which is allowed to harden into a mould shell. The pattern is then removed typically by steam and whereafter the melt is produced by means of vacuum induction melting (VIM), poured into the mould shell and allowed to solidify. Finally, the mould is destroyed to recover

the casting [6], [7]. Generally, HIP is applied to close any micro shrinkage from the casting process and to homogenize the material. The HIP treatment temperature for cast Alloy 718 is decided in order to avoid incipient melting of the γ -Laves eutectic, which has the lowest melting temperature of all constituents in the material. The two most common HIP treatment temperatures for cast Alloy 718 in the aerospace industry are 1120°C [8] and 1190°C [9], [10], which are below and above the incipient melting temperature of the γ -Laves eutectic constituent in the alloy, respectively, [9]. At the current state, there is no standardized HIP treatment available for Cast ATI® 718Plus™. The similar temperature for the γ -Laves eutectic formation as for Alloy 718 at about 1160°C [11] and the need for unified heat treatment from industrial perspective led to the choice of the same HIP solution temperatures for cast ATI® 718Plus™ as for cast Alloy 718. The HIP treatments at 1120°C and 1190°C at pressure of 100 MPa have shown to be effective in closing the porosity to similar extent for the two superalloys [12]. In the present study, pseudo-HIP treatments were applied to cast ATI® 718Plus™ in a regular laboratory furnace to analyse the effect of homogenization without any influence from pressure. Careful control of the grain size is one very important tool for controlling the mechanical properties of superalloys. Small grain size is considered beneficial for tensile and fatigue properties. Conversely, large grain size is favourable for creep strength. Therefore, grain size should be carefully controlled according to the specific application. In wrought materials this is preferably done by precipitating η or δ phase along the grain boundaries, which provides grain size in the range of 10 to 200 μm [13]. However, in castings, grain size values can reach up to 3 mm [14]. One way to keep small grain size values is by utilizing the Microcast-X process, which involves the careful control of pouring temperature and induced turbulence in the molten metal [6]. As a result, this can give grain sizes in the range of 90 to 1600 μm , which is significantly lower than for conventional castings [14]. When it comes to weldability, several studies have attributed a positive role to small grain size in limiting hot cracking susceptibility, supposed to be a result of larger grain boundary area available for stress accommodation [12–14].

3. Hot Cracking

Hot cracks are defined as cracks that occur during welding owing to the presence of liquid in the microstructure and they are differentiated between cracks occurring in the fusion zone (FZ) and heat affected zone (HAZ), respectively, namely solidification cracks and heat affected zone liquation cracks. The main theories covering hot cracking phenomena are summarised below.

3.1. Solidification cracking

Pumphrey et al. [18] proposed the so called “Shrinkage Brittleness Theory” in order to explain the cracking mechanism during casting and welding of Al. It was postulated that a brittle temperature range (BTR) exists for which the material is susceptible to cracking because it exhibits low ductility. This BTR has an upper limit named the coherent temperature, which is the temperature at which the growing dendrites come into mutual contact by forming a solid-coherent network, whereas the lower limit is defined by the solidus temperature. The BTR range is primarily influenced by the composition of the alloy.

Pellini [19] formulated the “Strain theory” based on the research performed to investigate hot tearing in castings and later adapted the same theory also to welding. The strain theory premises the presence of liquid films close to the solidus temperature. Their presence at the grain boundaries is the main cause of reduced ductility due to the low stress required for film separation. According to the strain theory, hot cracks cannot form in the so-called mushy zone, because of the ability of the liquid to flow and heal the cracks.

The “Generalized theory” by Borland [20], Figure 1, combines the previously mentioned theories but with some modifications. First of all, Borland separates the solidification range into four stages:

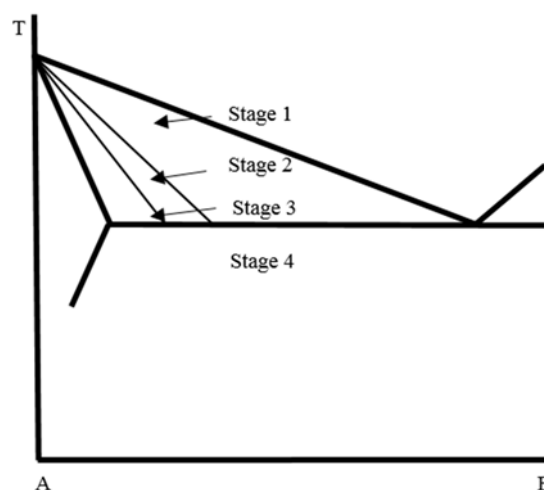


Figure 1. Solidification stages according to Borland’s Generalized theory. Figure adapted from [20]

Stage 1, where primary dendrites form as the temperature drops below the liquidus.

Stage 2, where the dendrites interlock by forming a solid network. In this stage, only the liquid is capable of movement between the dendrites.

Stage 3, where the grain development occurs. Here, the liquid is not capable of free movement because of the continuous network.

Stage 4, where all the liquid has solidified.

According to Borland, cracks can form in Stage 2 once an “almost continuous” network of dendrites has formed. In this stage, healing is possible since there is sufficient amount of liquid which can backfill the incipient cracks. He also defined the “critical solidification range” (CSR) to be associated with Stage 3, which is when a significant amount of cracking can occur, as the confinement of liquid to interdendritic areas without the ability to move freely occurs, which in turn inhibits healing of cracks. A wider CSR promotes a larger temperature range over which liquid is present, and hence the susceptibility towards cracking increases. In Stage 4, cracking is no longer possible as the material is fully solidified.

Matsuda et al. [21] proposed a modified concept of solidification cracking in reference to Borland’s “Generalized theory” based on experiments which allowed the direct observation of weld cracking through a high speed camera. Based on their observations, Stage 1 and Stage 2 defined by Borland, were shifted towards the liquidus. Moreover, Stage 3 was divided into “film stage” 3(h) and “droplet stage” 3(l), see Figure 2. Crack initiation can occur in the liquid film stage and propagate in the droplet stage, however, initiation is not possible in the latter due to the extensive solid-solid bridging.

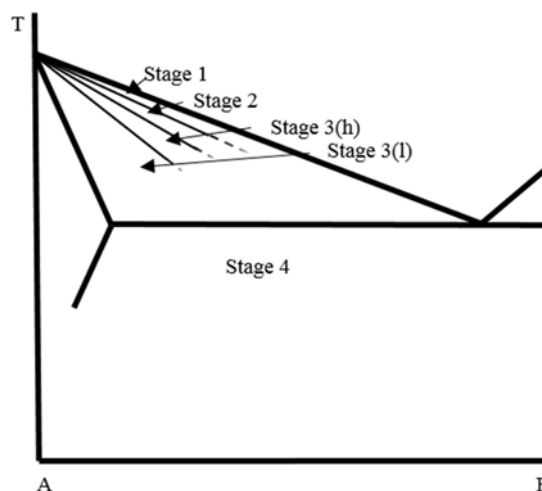
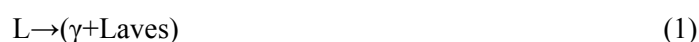


Figure 2. Solidification stages according to Matsuda et al. Figure adapted from [21]

All the theories agree upon the fact that weld solidification cracking derives from a combination of metallurgical factors and local strains at the final stages of solidification in the presence of some liquid

phase along the solidification boundaries. The solidification range is considered among the most important factor in determining the solidification cracking susceptibility. Generally, the lower the solidification temperature, the wider the temperature range at which the liquid will exist and this can aggravate the cracking tendency [15], [22]. Other important metallurgical factors are the amount and distribution of liquid at the final stages of solidification and grain boundary wetting. Cracking is enhanced when the surface tension of the liquid is low and continuous thin liquid films wet the grain boundaries. When a sufficient amount of terminal liquid is present the liquid has the ability to flow back into the cracks and heal them. The backfilling effect is especially relevant in alloys which solidify by a eutectic reaction such as cast Alloy 718 and cast ATI® 718Plus™. The solidification sequence in these alloys terminates by the following eutectic reaction [23]:



The γ -Laves eutectic reaction occurs at a temperature below the solidus of the γ phase, thus, it is responsible for extending the solidification range. The simulated and experimental values of the solidification temperature ranges for the two alloys are summarised in Table 2. Figure 3 shows an example of a solidification crack surrounded by high amount of γ -Laves eutectic constituents.

Table 2. Solidification results for cast ATI® 718 Plus™ and cast Alloy 718. Temperatures values are in °C (Paper II)

	JMatPro			DSC		
	T _{liquidus}	T _{solidus}	Sol. range	T _{liquidus}	T _{solidus}	Sol. range
Cast ATI® 718 Plus™	1328	1120	208	1328	1162	166
Cast Alloy 718	1357	1090	267	1334 [5]	1157 [5]	177 [5]

There are two views on the effect of base metal condition on the susceptibility towards solidification cracking. It is believed that melting and solidification in the fusion zone eliminate the thermal history of the alloy [24], which makes the solidification cracking independent of the base metal condition. On the other hand, it is believed that the weld metal grain size being a function of the base metal grain size due to the epitaxial growth which consequently can influence the susceptibility towards cracking [25]. Fine weld grain structure is considered less susceptible to cracking than coarse grain structure owing to better accommodation to strain [15]. The weld pool shape is also considered to be an important factor. When welding at high speed, centreline cracks can form as a result of the tear shaped weld pool, which creates an abrupt angle with the columnar grains forming from the two sides of the fusion line. This is not a concern when welding at low speeds; elliptical shaped welds lead to a smooth transition of the columnar grains at the weld centre [22].

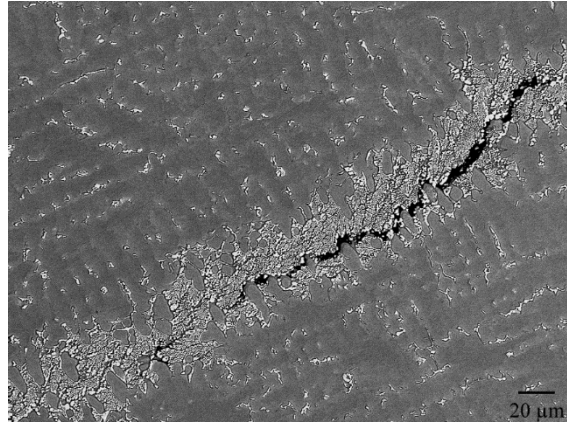


Figure 3. A solidification crack in Cast ATI® 718Plus™ (Paper II)

3.2. Heat affected zone liquation cracking

The mechanisms associated with the formation of HAZ liquation cracks are referred to as “liquation”. As the HAZ does not experience temperatures above the matrix solidus, liquid can only form if the melting point is locally suppressed by solute segregation or by the significant presence of secondary phase constituents. The formation of liquid films at grain boundaries lower the ductility locally, thus, increases the susceptibility towards cracking when a critical strain is exceeded. The phases or segregating elements responsible for crack formation vary from alloy to alloy.

The liquation of the grain boundaries leading to HAZ cracking can occur in two ways; segregation mechanism and penetration mechanism. The segregation mechanism occurs when solute or impurity elements segregate at the grain boundaries by diffusion mechanism to suppress the local melting temperature and thus leading to grain boundary melting. The presence of P, S and B at the grain boundaries is known to promote liquation cracking in Ni-based superalloys. In the penetration mechanism, the cracking occurs when a moving grain boundary intersects a locally melted region. The penetration mechanism is possible in two ways; one by constitutional liquation and the other by eutectic melting [15], [26]. The constitutional liquation mechanism was proposed by Pepe and Savage [27] for maraging steel weldments. The constitutional liquation involves melting including secondary phase constituent present in the HAZ of the base metal. The melting can occur at any temperature between the eutectic and the equilibrium solidus of the alloy. The liquid formed is a result of the interaction of the secondary phase compound with the surrounding matrix to form a low melting phase. The heating rate has to be rapid enough to get liquid phase below the equilibrium solidus of the alloy. By assuming a spherical precipitate and considering a heating rate to avoid equilibrium conditions, the phenomenon can be explained by considering Figure 4.

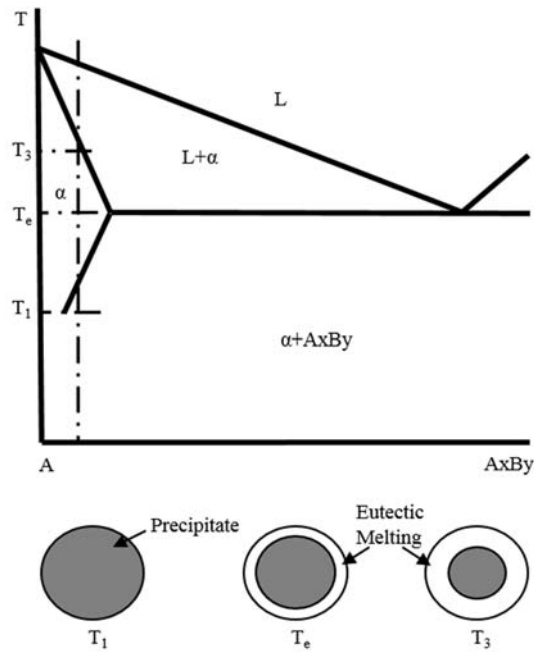


Figure 4. Schematic phase diagram and figure showing constitutional liquation. Adapted from [17]

Below the equilibrium eutectic temperature T_e , the precipitate does not experience any phase transformation. As the temperature reaches T_e , a eutectic liquid film forms at the interface between the particle and the matrix. As the temperature is increased above the eutectic point, the amount of melting will increase. Figure 5 shows a scanning electron microscope (SEM) image of a constitutional liquated carbide in the HAZ of cast ATI[®] 718 Plus[™].

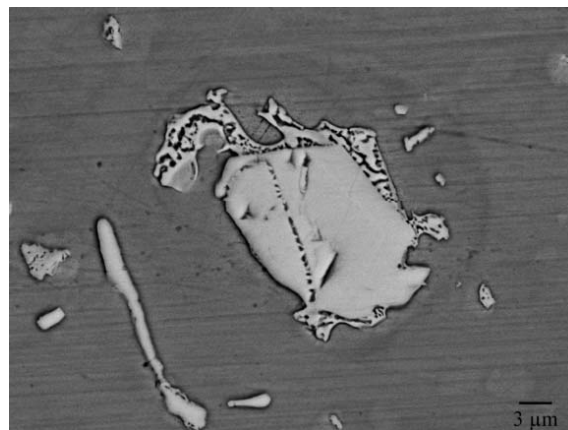


Figure 5. Constitutional liquation of a carbide in cast ATI[®] 718 Plus[™]

The mechanism of eutectic melting is typical for cast materials. The interdendritic regions melt at a lower temperature than the surrounding matrix. During welding the very rapid heating cycles do not allow the eutectic constituents to dissolve, whereby melting occurs when the eutectic temperature is exceeded [15], [26]. A HAZ liquation crack following this mechanism is shown in Figure 6.

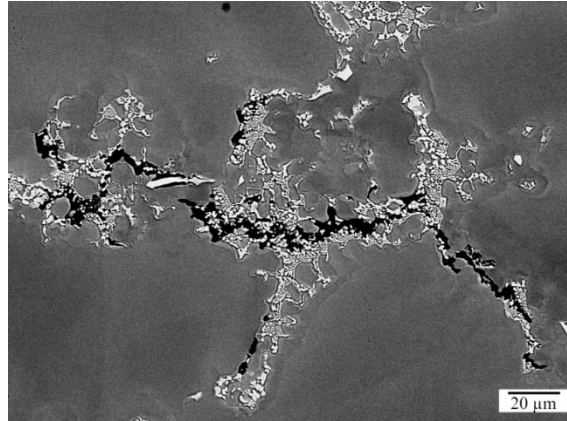


Figure 6. HAZ crack due to liquation of Laves eutectic in Alloy 718 (Paper I)

The following are the liquation mechanisms reported for Ni-based superalloys [5], [27], [28]:

- Constitutional liquation of secondary phases
- Melting of the matrix
- Liquation of precipitation hardening phases
- Melting of residual eutectic in cast material
- Segregation induced liquation

4. Experimental Methods

4.1. Materials and heat treatments

The composition of the cast Alloy 718 and cast ATI 718[®] Plus[™] being used in the current study is presented in Table 3. The details of the heat treatments are disclosed in Table 4.

Table 3. Composition of cast Alloy 718 and Cast ATI[®] 718 Plus[™] in wt%

Element	Cast Alloy 718	Cast ATI 718 [®] Plus [™]
Ni	53.0	Bal.
Cr	18.1	20.5
Fe	Bal.	9.7
Co	0.07	8.3
Nb	5.3	6.3
Mo	3.0	2.7
Al	0.42	1.5
Ti	0.99	0.80
C	0.05	0.05
W	0.01	1
Mn	0.03	0.01
Cu	0.01	0.1
Si	0.07	0.03
P	0.009	0.008
B	0.03	0.005

Table 4. Heat treatment steps for cast Alloy 718 and cast ATI[®] 718 Plus[™]

Material	HIP/Pseudo-HIP	Post-HIP in vacuum	Solution heat treatment
Cast Alloy 718	HIP-1120°C/4h [8]	1050°C/1h + FC to 650°C in 1h	950°C/1h + AC
	HIP-1190°C/4h [9], [10]	870°C /10h + FC to 650°C in 1h	950°C/1h + AC
Cast ATI [®] 718Plus [™]	1120°C/4h and 24h + WQ	-	-
	1160°C/4h + WQ	-	-
	1190°C/4h and 24h + WQ	-	-

FC=furnace cooling, AC=air cooling, WQ=water quenching

Cast Alloy 718 was subjected to HIP treatments of 1120°C/4h and 1190°C/4h at 100 MPa followed by post-HIP at 1050°C/1h and 870°C/10h, respectively, utilizing controlled cooling in the furnace to 650°C, followed by a solution heat treatment at 950°C/1h. Cast ATI® 718 Plus™, on the other hand, was subjected to heat treatments at three different temperatures of 1120, 1160 and 1190°C for dwell times of 4h and 24h, followed by water quenching. Besides the heat treated conditions, the as cast version for each alloy was also tested as reference.

4.2. Vareststraint weldability testing

Cast plates in the different heat treated conditions were electric discharge machined into test plates with approximate dimensions of 150 x 60 x 3.3 mm. The Vareststraint testing equipment is shown in Figure 7 together with a closer look of the testing set up in Figure 8.

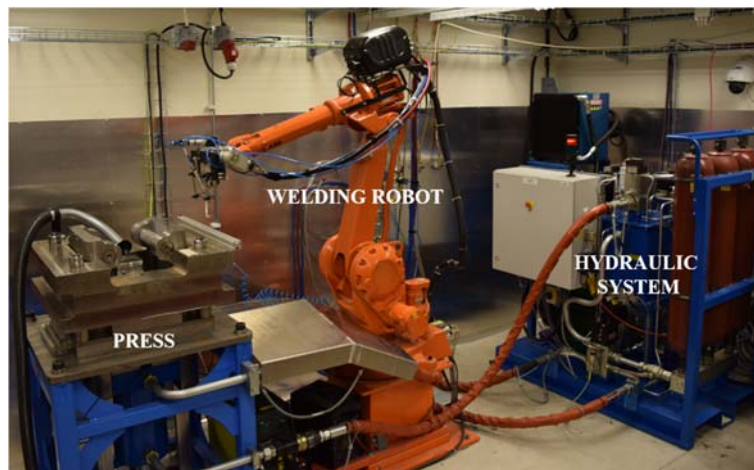


Figure 7. Vareststraint weldability testing equipment

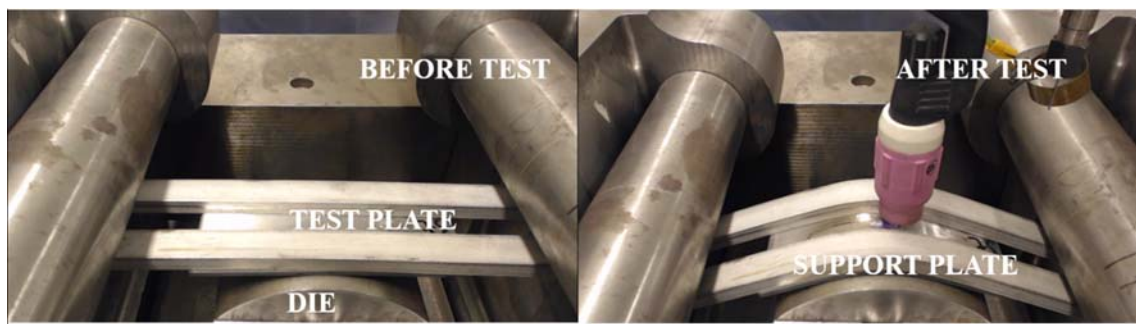


Figure 8. Testing set up, before (left) and after (right) Vareststraint test

Bead on plate welding was performed longitudinally to the plate direction at test radii from 20 to 200 mm, which corresponded to augmented strain levels of 0.8, 1.1, 1.6, 2.1, 2.7, 3.3, 3.9 and 8.2%. By knowing the die radius (R) and the thickness of the test plate (t), the strain (ϵ) is given by:

$$\epsilon = \frac{t}{2R} \quad (2)$$

Varestraint testing and GTAW (Gas tungsten arc welding) parameters are summarised in Table 5. The selected parameters are based on a previous DOE (design of experiments) study on Varestraint testing, which produced the least amount of scatter [29].

Table 5. Parameters used for longitudinal Varestraint weldability testing using GTAW

Welding Speed (mm/s)	Stroke Rate (mm/s)	Welding Current (A)	Arc length (mm)	Ar gas flow (l/min)
1	10	70	2	15

In **Paper I** (Hot cracking in cast Alloy 718) 7 plates for each condition and strain level were tested, 168 test plates in total. In **Paper II** (Varestraint weldability testing of cast ATI[®] 718 Plus[™] – A comparison to cast Alloy 718), testing was performed at strain levels of 1.1, 1.6, 2.1, and 2.7% with three test plates for each strain level and condition having a total of 72 test plates.

4.3. Sample preparation and characterization

After Varestraint testing, oxide layers were removed by Carbimet[™] polishing paper. Crack measurements were conducted by using Olympus SZX 9 stereo microscope at 57x magnification.

4.3.1. Metallographic preparation

Base metal and weld cross-sections were cut out from the test plates. The metallographic preparation steps are summarised as follows:

- Mounting using conductive and thermoplastic compounds with Buehler Simpliment 2000
- Grinding steps of 125 µm and 45 µm discs with Buehler PowerPro 5000
- Polishing steps with Buehler Hercules S rigid disc using 9µm Kemet liquid diamond and with Trident cloth disc using 3µm Kemet liquid diamond
- Electrolytic etching using oxalic acid ad 3.2 V for 1-2 minutes of time.

4.3.2. Grain size analysis

Grain size analysis was carried out according to the ASTM E112 standard [30]. Grain size measurements for the cast Alloy 718 followed the metallographic steps previously described with the only difference being associated with the type of etchant. Kalling's 2 reagent (2 g CuCl₂, 49 mL HCl, 40-80 mL ethanol) was used for grain size evaluation. For cast ATI[®] 718Plus[™], grain size evaluation was conducted on macro etched samples with 90% HCl, 10% HNO₃ and 120 g/L FeCl₃ powder heated to about 50°C.

4.3.3. Microstructural characterization

Microstructural characterization was conducted using an Olympus BX60M optical microscope and a LEO 1550 FEG-SEM equipped with Oxford Electron Dispersive X-ray Spectrometer.

4.3.4. Hardness testing

Hardness measurements were conducted by using Shimadzu HVM-2 micro hardness testing machine with a force of 0.5 kgf (HV0.5).

4.3.5. Differential scanning calorimetry

Differential Scanning Calorimetry (DSC) was performed by using a Netzsch-STA 409 PC Luxx simultaneous DSC-TG equipment using heating and cooling rates of 20°C/min at soak temperature of 1400°C.

4.3.6. Material modelling

JMatPro 8.0 in conjunction with the Ni-based superalloy database was used to model the phase stability of the investigated alloys.

5. Summary of Appended Papers

5.1. Hot cracking in cast Alloy 718 (Paper I)

In **Paper I**, the effect of two HIP treatments on hot cracking of cast Alloy 718 were studied in reference to the as-cast condition. A wide scatter in average total crack length (Avg. TCL) values were found for both solidification cracking (Figure 9) and HAZ liquation cracking (Figure 10). Despite the large scatter in results, which is typical for cast materials, the overall conclusion was that no distinction in solidification cracking susceptibility existed considering the different base metal conditions. On the other hand, regarding HAZ liquation cracking, the as-cast condition exhibited the least amount of cracking, followed by HIP-1120 and HIP-1190 conditions.

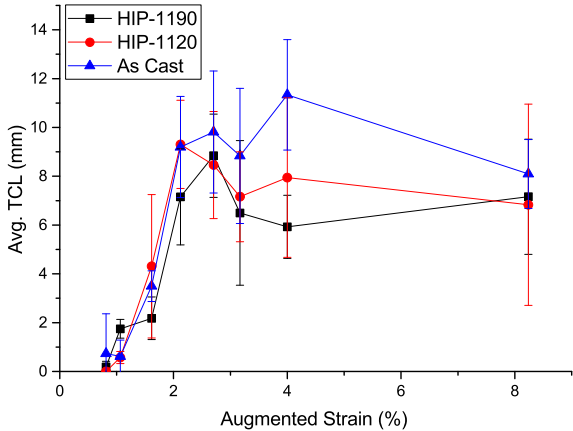


Figure 9. FZ cracking response with standard deviations for the as-cast, HIP-1120 and HIP-1190 conditions

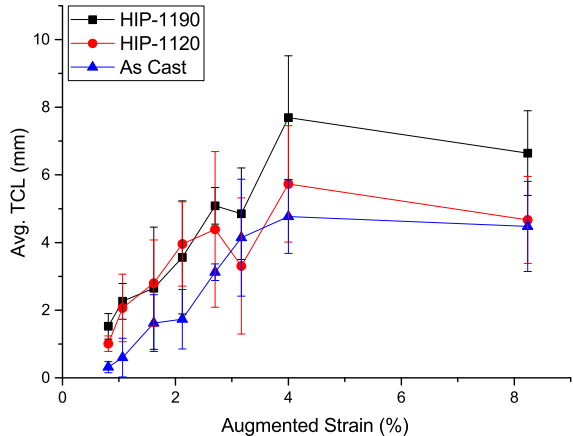


Figure 10. HAZ liquation cracking response with standard deviations for the as-cast, HIP-1120 and HIP-1190 conditions

Small and discontinuous cracks associated with melting of the γ -Laves eutectic phase were found in the as-cast condition (Figure 11), which showed the most extensive segregation, about 3.7% in terms of volume fraction (Vv) of secondary precipitates, but minimum average grain size value of about 1.7mm (Table 6). After the HIP treatments, the main effects in the base metal were seen to be an improved homogenization and an increase of grain size but with slight reduction of hardness (Table 6). The estimated Vv for the HIP-1120 condition was about 1.7% and the grain size was about 2.6mm, whereas the Vv in HIP-1190 was about 1.3% and the grain size was about 3.3mm. For both HIP conditions, the cracking occurred along the grain boundaries due to the grain boundary liquation mechanism. In particular, the grain size increase allowed for longer cracks to propagate in relation to the lower grain size condition as shown in Figure 11. Larger grain size is generally known to be detrimental in terms of hot cracking susceptibility [15]–[17], [31] and this was found to be an important factor in differentiating the cracking susceptibility between the two HIP conditions.

Table 6. Volume fraction of secondary precipitates, grain size measurements and base metal hardness in cast Alloy 718

Condition	Vv (%)	GS (mm)	HV
As-Cast	3.7±0.6	1.7 ±0.1	260±20
HIP-1120	1.7±0.1	2.6±0.3	220±30
HIP-1190	1.3±0	3.3±0.3	210±20

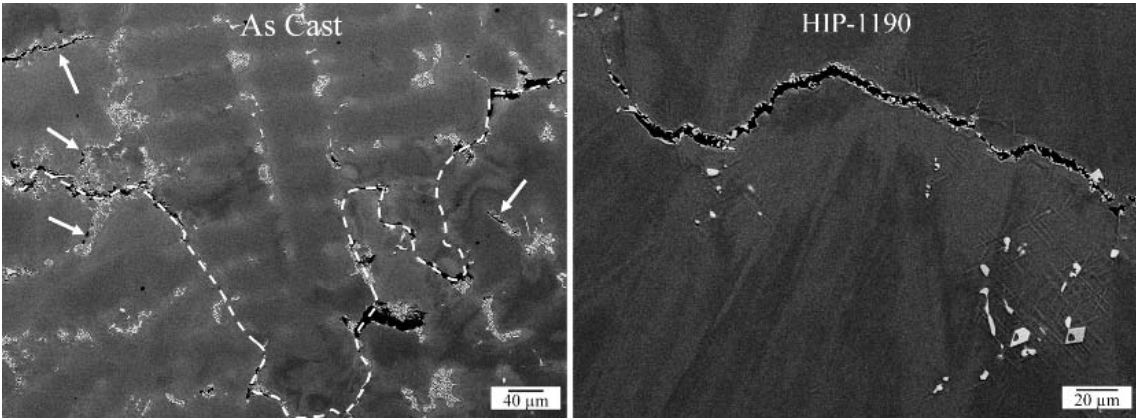


Figure 11. Cracks formed in the liquated regions in the as cast condition to the left. Liquation cracking in the HIP-1190 condition of cast Alloy 718 to the right

5.2. Vareststraint weldability testing of cast ATI® 718 Plus™ – A comparison to cast Alloy 718 (Paper II)

This study focused on the effect of the pseudo-HIP treatments at temperatures of 1120°C, 1160°C and

1190°C and dwell heat treatment times of 4h and 24h in reference to the as cast condition, on hot cracking of cast ATI® 718Plus™. Moreover, a comparison of weldability to the cast Alloy 718 from **Paper I** was also evaluated.

No difference was seen in terms of solidification cracking susceptibility; for all conditions the average total crack length (TCL) as function of augmented strain was similar, see Figure 12 left. However, regarding HAZ liquation cracking, the heat treatments at longer dwell times at 1120 and 1190°C for 24h exhibited the most extensive cracking, whereas those at 1120, 1160 and 1190°C at short dwell time of 4h exhibited the least amount of cracking, see Figure 12 right. The average TCL for the as-cast condition had an intermediate behaviour.

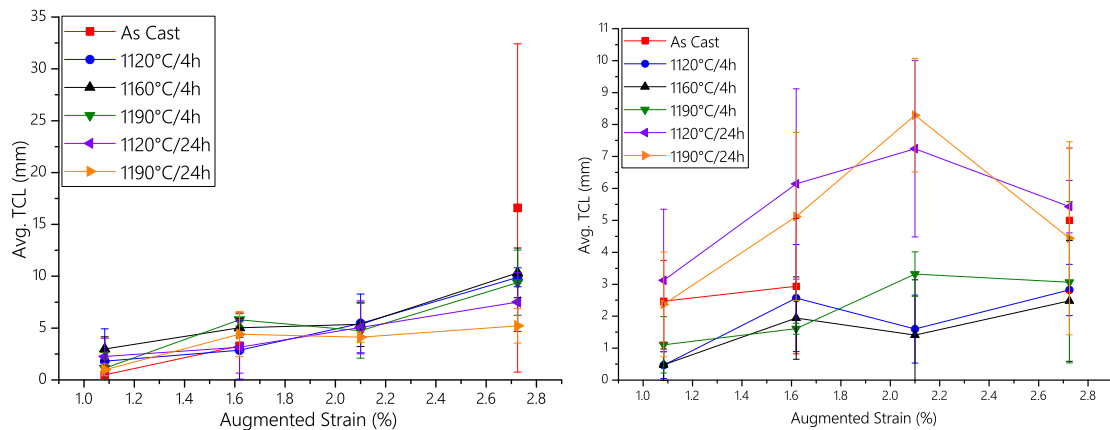


Figure 12. Solidification cracking susceptibility to the left. Heat affected zone liquation cracking of cast ATI® 718Plus™ to the right

The as-cast base metal condition exhibited the most extensive segregation and the highest hardness value of about 375 HV. After the pseudo-HIP treatments, the amount of Laves phase reduced significantly and the hardness values dropped to between 170-180 HV. Contrary to what is usually expected, grain growth did not occur; the average grain size values were similar for all the conditions including the as-cast except for the condition 1190°C/4h, which exhibited smaller grain size value of about 1.7 mm in relation to about 2.3 mm for the other conditions (Table 7).

Table 7. Volume fraction of Laves phase, base metal hardness and grain size values for the different conditions of cast ATI® 718Plus™

	As-Cast	1120°C/4h	1120°C/24h	1160°C/4h	1190°C/4h	1190°C/24h
V_v (%)	4.1±0.7	0.3±0.2	0.1±0.1	0.1±0.1	0.0±0.0	0.0±0.0
HV	375±15	170±0	180±0	170±5	170±0	180±5
GS (mm)	2.3±0.5	2.2±0.5	2.4±0.5	2.3±0.4	1.7±0.4	2.5±0.6

Further analysis revealed that the grain size differed significantly within the cast test plates, as shown in

Figure 13. Grain size values varied from about 1.3 mm to about 3.2 mm from one end to another end of the plate. The grain size measurements were taken at the location where the largest plastic deformation occurred during the Varestraint test. Using a specified location on the plates makes the measurement very sensitive to local changes in grain size, which is a common observation in cast material and can explain the observed smaller average grain size of the 1190°C/4h plates. Still, the reason behind the difference in cracking susceptibility between the heat treatments at different soak temperatures is not clear and this requires further investigation.

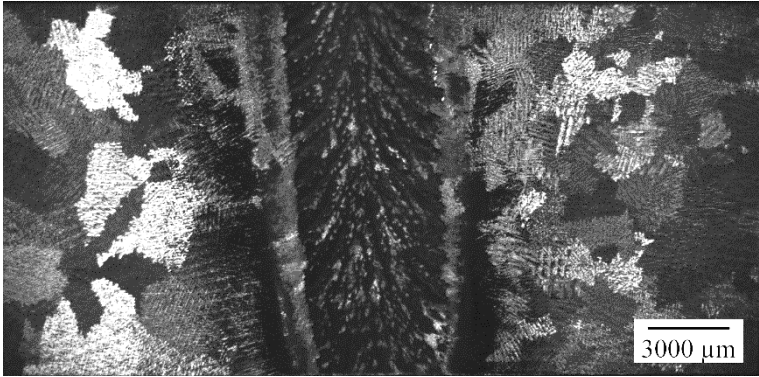


Figure 13. Grain structure in as-cast test plate

Solidification cracking susceptibility for the two alloys revealed no difference when comparing the as-cast conditions of Alloy 718 and ATI® 718 Plus™, Figure 14.

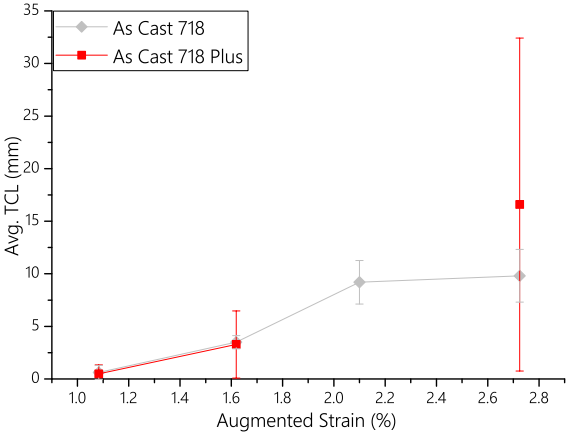


Figure 14. Solidification cracking susceptibility of the as cast conditions of Alloy 718 and cast ATI® 718Plus™

As-cast ATI® 718Plus™ exhibited higher cracking susceptibility in the HAZ than the as-cast Alloy 718, Figure 15. From Table 8, the volume fraction of secondary precipitates were similar, but the base metal hardness differed by about 100 HV.

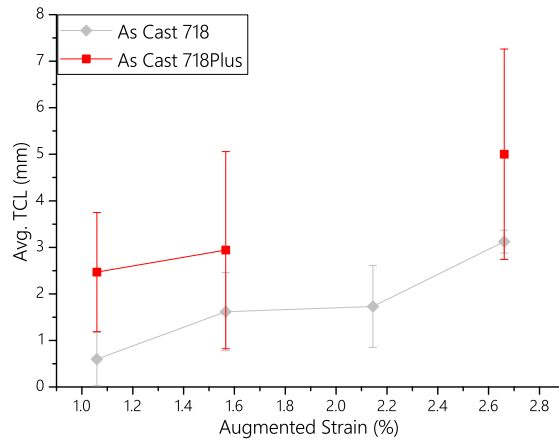


Figure 15. HAZ cracking susceptibility of as-cast Alloy 718 and as-cast ATI® 718Plus™

Interestingly, after the heat treatments, the cracking susceptibility of cast ATI® 718Plus™ was lower than that of cast Alloy 718, Figure 16.

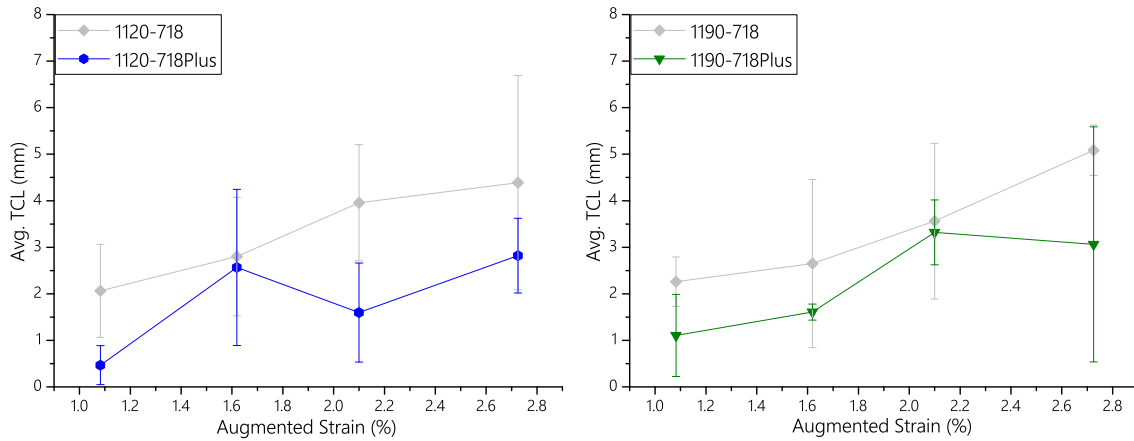


Figure 16. Comparison of HAZ cracking susceptibility after heat treatments at 1120°C to the left and after 1190°C to the right

Comparing the values in Table 8, it can be seen the volume fraction of secondary precipitates and hardness values were higher for cast Alloy 718 in the heat treated conditions but the average grain size was larger only for the HIP-1190 condition. Therefore, the synergetic effect of volume fraction, hardness and grain size seems to be involved when evaluating the difference in cracking susceptibility.

Table 8. Comparison of volume fraction of secondary precipitates, base metal hardness and grain size values for the different conditions of cast ATI® 718 Plus™ and cast Alloy 718

	Cast ATI® 718 Plus™			Cast Alloy 718		
	As-Cast	1120°C/4h	1190°C/4h	As Cast	HIP-1120	HIP-1190
Vv (%)	4.0±0.5	0.3±0.2	0.0±0.0	3.7±0.6*	1.7±0.1*	1.3±0*
HV	375±15	170±0	170±0	260±20	220±30	210±20
GS (mm)	2.3±0.5	2.2±0.5	1.7±0.4	1.7±0.1	2.6±0.3	3.3±0.3

* Volume fraction of Laves and NbC

The backfilling effect for the two superalloys was also quantified at two different strain levels, however, no difference was found.

6. Conclusions

- **Hot cracking in cast Alloy 718 (Paper I)**
 - Solidification cracking susceptibility of cast Alloy 718 was found to be independent of the heat treatment conditions.
 - The as-cast condition showed the least amount HAZ liquation cracking followed by HIP-1120 and HIP-1190.
 - The amount of secondary phase precipitates and the grain size were found to influence the cracking susceptibility.
- **Varestraint weldability testing of cast ATI[®] 718 Plus[™] – A comparison to cast Alloy 718 (Paper II)**
 - No difference in solidification cracking of cast ATI[®] 718 Plus[™] was seen in between the different heat treatment conditions.
 - The HAZ liquation cracking was found to be related to the heat treatment dwell time rather than soak temperature. The heat treatments at 1120 and 1190°C of 24h dwell time resulted in more extensive cracking than the 1120, 1160 and 1190°C of 4h dwell time.
 - The as-cast condition was found to be more crack susceptible than the heat treatments at 4h but less susceptible than those at 24h.
 - The cast ATI[®] 718Plus[™] and Alloy 718 had similar solidification cracking susceptibility.
 - The as-cast condition of ATI[®] 718Plus[™] exhibited higher amount of heat affected zone cracking than the as-cast Alloy 718.
 - After the heat treatments at 1120 and 1190°C for 4h, the cracking was reduced in the cast ATI[®] 718 Plus[™] in reference to that of cast Alloy 718.
 - There were no difference in backfilling among the two alloys.

7. Future Work

Hot cracking will be investigated for another cast Ni-based superalloy, Haynes[®] 282[®]. Further focus will be on advanced characterization of the Vareststraint-tested cast superalloys, Alloy 718, ATI[®] 718Plus[™] and Haynes[®] 282[®] in terms of microstructural changes after the heat treatments, metallurgical reactions occurring during welding and analyses of precipitates involved in cracking.

8. Acknowledgements

I would like thank my supervisor Assoc. Prof. Joel Andersson for his continuous support throughout this journey. I would also like to thank my examiner Prof. Lars Nyborg for the support provided through the project.

Special thanks to my friends and colleagues in Trollhättan and Göteborg for making this journey even more fun!

Last but not least, thanks to my parents, my sisters, Loveneet and Mehak for the support!!! ♥

Eternal love to the Guru,

The King of the Kings

References

- [1] EISELSTEIN, H.L. Age-hardenable nickel alloy. U.S. Patent No 3,046,108, 1962.
- [2] BALLOU, O. W.; COFFEY, M. W. History of Cast Inco 718. *Superalloys 1988*, 1988, 469-473.
- [3] W. D. Cao and R. Kennedy, Role of chemistry in 718-type alloys–Allvac® 718Plus™ alloy development, in *Superalloys 2004*, 2004, pp. 91–99.
- [4] B. Peterson, D. Frias, D. Brayshaw, R. Helmink, S. Oppenheimer, E. Ott, R. Benn, and M. Uchic, On the Development of Cast ATI 718Plus® Alloy for Structural Gas Turbine Engine Components, in *Superalloys 2014 Conference*. TMS, 2012.
- [5] J. Andersson, Weldability of precipitation hardening superalloys–influence of microstructure. Phd Thesis, Chalmers University of Technology, 2011.
- [6] SIMS, C.T.; STOLOFF, N.S.; HAGEL, W.C. *Superalloys II*. Wiley-Interscience, 1987.
- [7] M. J. Donachie and S. J. Donachie, *Superalloys: a technical guide*. ASM International, 2002.
- [8] M.L. Barron, Crack Growth-Based Predictive Methodology for the Maintenance of the Structural Integrity of Repaired and Nonrepaired Aging Engine Stationary Components. GE AIRCRAFT ENGINES CINCINNATI OH, 1999.
- [9] S. M. Snyder and E. E. Brown, SNYDER, S.M.; BROWN, E.E. Laves free cast + hip nickel base superalloy. U.S. Patent No 4,750,944, 1988.
- [10] D. F. Paulonis and J. J. Schirra, Alloy 718 at Pratt & Whitney–Historical perspective and future challenges. *Superalloys*, 2001, 718.625,706: 13-23.
- [11] S. Singh and J. Andersson, Varestraint weldability testing of cast ATI® 718 Plus™ – A comparison to cast Alloy 718, Submitted for Journal Publication.
- [12] J. Andersson, F. Vikström, and B. Pettersson, HIP-Densification of Alloy 718 and ATI 718Plus®, in 8th International Symposium on Superalloy 718 and Derivatives, 2014.
- [13] J. Jacobsson and J. Andersson, Weldability of Superalloy Alloy 718 and ATI® 718Plus™ - A study performed with Varestraint Testing, *Materials Testing*, vol. 59.9, pp. 769–773, 2017.
- [14] X. Huang, N. L. Richards, and M. C. Chaturvedi, Effect of Grain Size on the Weldability of Cast Alloy 718, *Materials and Manufacturing Processes*, vol. 19, no. 2, pp. 285–311, Dec. 2004.
- [15] DUPONT, J.N.; LIPPOLD, J.C.; KISER, S.D. *Welding metallurgy and weldability of nickel-base alloys*. Hoboken, N.J: John Wiley & Sons, 2009.
- [16] R. G. Thompson, J. J. Cassimus, D. E. Mayo, and J. R. Dobbs, The relationship between grain size and microfissuring in alloy 718. *Welding journal*, 1985, 64.4: 91-96.
- [17] I. Woo, K. Nishimoto, K. Tanaka, and M. Shirai, Effect of grain size on heat affected zone cracking susceptibility. Study of weldability of Inconel 718 cast alloy (2nd Report), *Welding International*, vol. 14, no. 7, pp. 514–522, Jan. 2000.
- [18] PUMPHREY, W. I.; JENNINGS, P. H. A consideration of the nature of brittleness at temperatures above the solidus in castings and welds in aluminium alloys. *Journal of the Institute of Metals*, 1948, 75.4: 235-&.
- [19] PELLINI, W.S. Strain theory of hot tearing., *Foundry*, vol. 80, no. 11, pp. 125–133, 1952.
- [20] J. Borland, Generalized theory of super-solidus cracking in welds (and castings), *British Welding Journal* 7.8, pp. 508–512, 1960.
- [21] F. Matsuda, H. Nakagawa, and K. Sorada, Dynamic Observation of Solidification and Solidification Cracking during Welding with Optical Microscope (I): Solidification Front and Behavior of Cracking (Materials, Metallurgy & Weldability), *Transactions of JWRI*, vol. 11.2, pp. 67–77, 1982.
- [22] S. Kou, *Welding metallurgy*, 2nd ed. Hoboken, N.J: Wiley-Interscience, 2003.
- [23] J. N. DuPont, C. V. Robino, and A. R. Marder, DUPONT, J. N.; ROBINO, C. V.; MARDER, A. R. Solidification and weldability of Nb-bearing superalloys. *Welding Research Supplement*, 1998. 417-431., *Welding Journal*, 1998.
- [24] CIESLAK, M. J.; HEADLEY, T. J.; FRANK, R. B. The welding metallurgy of custom age 625 PLUS alloy. *Welding Journal*, 1989, 68.12: 473-482.
- [25] K. Shinozaki, P. Wen, M. Yamamoto, K. Kadoi, Y. Kohno, and T. Komori, Effect of grain size on solidification cracking susceptibility of type 347 stainless steel during laser welding, 2010.

- [26] J. C. Lippold, *Welding metallurgy and weldability*. Hoboken, New Jersey: John Wiley & Sons Inc, 2015.
- [27] J. J. Pepe and W. F. Savage, Effects of constitutional liquation in 18-Ni maraging steel weldments (Microsegregation and grain boundary liquation in heat affected zone of 18-Ni maraging steel welds), *WELDING JOURNAL, RESEARCH SUPPLEMENT*, vol. 46, 1967.
- [28] M. C. Chaturvedi, Liquation Cracking in Heat Affected Zone in Ni Superalloy Welds, *Materials Science Forum*, vol. 546–549, pp. 1163–1170, 2007.
- [29] J. Andersson, J. Jacobsson, and C. Lundin, A Historical Perspective on Varestraint Testing and the Importance of Testing Parameters. In: *Cracking Phenomena in Welds IV*. Springer International Publishing, 2016. 3-23.
- [30] ASTM, E112-96. 112–96. Standard Test Methods for Determining Average Grain Size. ASTM International, 2004. .
- [31] HONG, J.K.; PARK, J.H.; PARK, N.K.; EOM, I.S.; KIM, M.B.; KANG, C.Y. Microstructures and mechanical properties of Inconel 718 welds by CO₂ laser welding, *Journal of Materials Processing Technology*, vol. 201, no. 1–3, pp. 515–520, May 2008.